

Fhl2 deficiency results in osteopenia due to decreased activity of osteoblasts

Thomas Günther¹, Cecilia Poli¹, Judith M Müller¹, Philip Catala-Lehnen^{2,3}, Thorsten Schinke^{2,3}, Na Yin¹, Sandra Vomstein¹, Michael Amling^{2,3} and Roland Schüle^{1,*}

¹Universitäts-Frauenklinik und Zentrum für Klinische Forschung, Klinikum der Universität Freiburg, Freiburg, Germany, ²Department of Trauma, Hand and Reconstructive Surgery, Hamburg University School of Medicine, Hamburg, Germany and ³Experimental Trauma Surgery and Skeletal Biology, Center for Biomechanics, Hamburg University School of Medicine, Hamburg, Germany

Osteoporosis is one of the major health problems today, yet little is known about the loss of bone mass caused by reduced activity of the bone-forming osteoblasts. Here we show that mice deficient for the transcriptional cofactor *four and a half LIM domains 2 (Fhl2)* exhibit a dramatic decrease of bone mass in both genders. Osteopenia is caused by a reduced bone formation rate that is solely due to the diminished activity of *Fhl2*-deficient osteoblasts, while their number remains unchanged. The number and activity of the bone-resorbing cells, the osteoclasts, is not altered. Enforced expression of *Fhl2* in differentiated osteoblasts boosts mineralization in cell culture and, importantly, enhances bone formation in transgenic animals. *Fhl2* increases the transcriptional activity of runt-related transcription factor 2 (*Runx2*), a key regulator of osteoblast function, and both proteins interact *in vitro* and *in vivo*. In summary, we present *Fhl2*-deficient mice as a unique model for osteopenia due to decreased osteoblast activity. Our data offer a novel concept to fight osteoporosis by modulating the anabolic activity of osteoblasts via *Fhl2*.

The EMBO Journal (2005) 24, 3049–3056. doi:10.1038/sj.emboj.7600773; Published online 4 August 2005

Subject Categories: chromatin & transcription; development

Keywords: bone formation; *Fhl2*; osteoblast; osteoporosis; *Runx2*

Introduction

The maintenance of an overall constant bone mass is achieved by a balance between bone matrix deposition and mineralization effected by osteoblasts and resorption caused by osteoclasts (Karsenty and Wagner, 2002). Bone loss is the outcome of imbalanced bone resorption relative to bone formation (Teitelbaum, 2000). Although impaired bone formation contributes to the pathogenesis of osteoporosis, our

knowledge of factors involved is limited. Characterization of the molecular mechanisms regulating bone formation is essential to understand the cause of osteoporosis. The runt-related transcription factor 2 (*Runx2*) is a master regulatory gene of osteoblast differentiation (Ducy *et al*, 1997; Komori *et al*, 1997; Lee *et al*, 1997; Mundlos *et al*, 1997; Otto *et al*, 1997), but also controls the activity of mature osteoblasts (Ducy *et al*, 1999).

FHL2 is a member of the LIM-only subclass of the LIM protein superfamily. LIM proteins are defined by the presence of one or more LIM domains that mediate protein–protein interaction (Kadmas and Beckerle, 2004). The members of the FHL subclass of LIM-only proteins consist of four-and-a-half LIM domains, exhibit a restricted expression pattern, and can function as transcriptional cofactors (Fimia *et al*, 2000; Müller *et al*, 2000; Labalette *et al*, 2004; Philippar *et al*, 2004; Yang *et al*, 2005). *FHL2* is highly expressed in the myocardium and in epithelial cells of the prostate (Chan *et al*, 1998; Müller *et al*, 2000). *FHL2* has been shown to act as a cofactor of several transcription factors, including androgen receptor (AR), CREB, AP-1, and SRF (Fimia *et al*, 1999; Müller *et al*, 2000; Morlon and Sassone-Corsi, 2003; Philippar *et al*, 2004). In addition, *FHL2* negatively regulates MAPK signaling in cardiomyocytes (Purcell *et al*, 2004). *FHL2* localizes to focal adhesions and translocates to the nucleus upon RhoA stimulation, thereby linking extracellular signals to gene expression (Müller *et al*, 2002). Heart development and function of *Fhl2*-deficient mice is normal (Chu *et al*, 2000), whereas in response to β -adrenergic stimulation *Fhl2*-deficient mice show a mild increase of heart hypertrophy (Kong *et al*, 2001). So far, this is the only phenotype observed in *Fhl2*-deficient mice, although *Fhl2* expression is not limited to heart.

The present analysis uncovers *Fhl2* expression in bone. *Fhl2*-deficient mice are osteopenic specifically due to decreased osteoblast activity. Conversely, enforced expression of *Fhl2* in mature osteoblasts of transgenic mice results in increased bone mass and, consequently, *Fhl2* regulates mineralization in a cell culture model system. On the molecular level, we show that *Fhl2* interacts with *Runx2* and functions as a transcriptional coactivator. Taken together, our data demonstrate a novel physiological function for *Fhl2* and opens the path for the development of anabolic drugs that maintain bone mass through the regulation of *Fhl2* activity in osteoblasts.

Results and discussion

Fhl2 is expressed in osteoblasts and *Fhl2*-deficient mice are osteopenic

To investigate the potential effect of *Fhl2* in bone, we analyzed *Fhl2*-deficient (*Fhl2*^{-/-}) mice. The targeting strategy led to introduction of the β -galactosidase reporter under the control of the endogenous *Fhl2* promoter (Kong *et al*, 2001). We used this gene to demonstrate *Fhl2* expression in bone *in situ* (Figure 1A, top left). We detected staining of the bone

*Corresponding author. Zentrum für Klinische Forschung, Molekulare Gynäkologie, Universitäts-Frauenklinik, Breisacherstr. 66, 79106 Freiburg, Germany. Tel.: +49 761 270 6310; Fax: +49 761 270 6311; E-mail: roland.schuele@uniklinik-freiburg.de

Received: 16 March 2005; accepted: 14 July 2005; published online: 4 August 2005

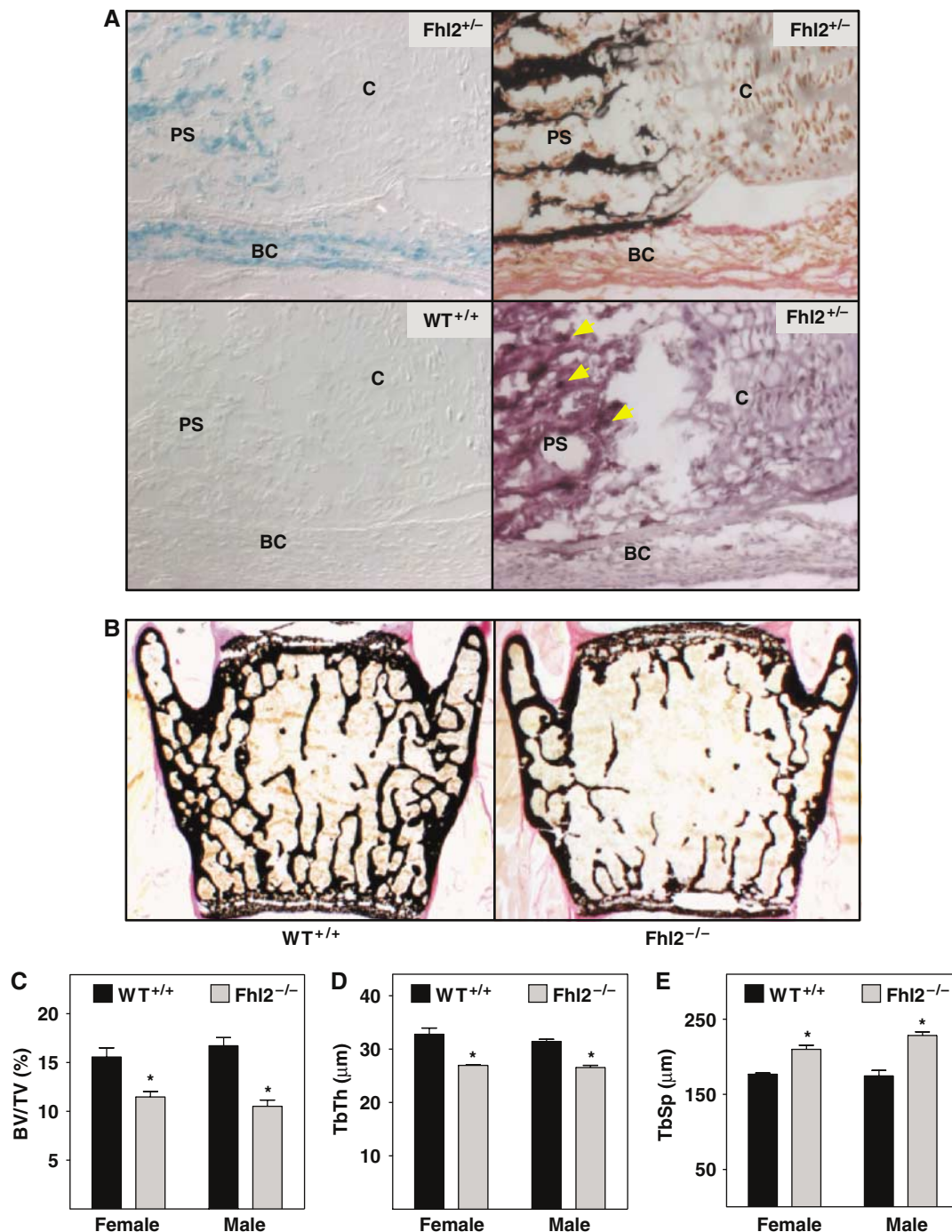


Figure 1 Osteopenia in *Fhl2*^{-/-} mice. (A) X-gal stain (blue) of the femur of a heterozygous newborn reveals specific *Fhl2* expression in the BC and PS (top left) compared to a C57BL/6 wild-type littermate (bottom left; C: growth plate cartilage). Von Kossa staining (black) identifies calcified extracellular matrix (top right) and Trap staining detects osteoclasts (bottom right, arrows). (B–E) Comparison of vertebrae from C57BL/6 and congenic *Fhl2*^{-/-} littermates by von Kossa stain (black, B) uncovers reduction of bone volume as a ratio of tissue volume (BV/TV) in mutant females and males (C), accompanied by reduced trabecular thickness (TbTh, D) and increased trabecular spacing (TbSp, E). Bars represent mean + s.d. ($n \geq 5$). *Statistically significant difference ($P < 0.05$).

collar (BC) region and the primary spongiosa (PS) of heterozygous mice, whereas no reporter gene expression was observed in growth plate cartilage (Figure 1A, top left) and in C57BL/6 wild-type littermate controls (Figure 1A, bottom left). The bone matrix is demarcated in black by von Kossa staining (Figure 1A, top right) and bone-resorbing cells are stained by Trap (Figure 1A, bottom right, arrows). Since the BC is devoid of osteoclasts, this pattern of expression suggests that *Fhl2* is expressed in bone-forming osteoblasts.

We performed histological analysis of bones of *Fhl2*^{-/-} mice at the age of 1 week, 1, 3, 6, and 9 months. Von Kossa staining, radiography, and micro-computed tomography analysis demonstrate that bone mass is progressively lost compared to wild-type control mice, leading to an osteopenic phenotype (Figure 1B and Supplementary Figure 1; data not shown). The growth of *Fhl2*^{-/-} mice is not affected (Supplementary Figure 1). Histomorphometric analysis of trabecular bone volumes corroborates the osteopenia of

Fhl2^{-/-} mice. *Fhl2*^{-/-} mice, 9-month old, show a marked reduction in bone mass by 32% compared to age- and sex-matched C57BL/6 wild-type control animals (Figure 1C). Bone loss is reflected by a decrease in trabecular thickness and an increase in trabecular spacing in *Fhl2*^{-/-} mice compared to control animals (Figure 1D and E). Taken together, both female and male *Fhl2*^{-/-} mice exhibit osteopenia to the same extent (Figure 1C–E).

Bone formation rate is reduced in *Fhl2*^{-/-} mice

To analyze the mechanism of *Fhl2* action, we first demonstrated that the number of osteoblasts and osteoclasts relative to the bone volume in *Fhl2*^{-/-} mice was not altered in comparison to C57BL/6 control littermates (Figure 2A). We then determined bone resorption *in vivo* by measurement of pyridinium crosslinks in urine samples. Pyridinium crosslinks are a degradation product of bone resorption released into the circulation and hence directly mirror osteoclast activity (Robins *et al*, 1991). As shown in Figure 2B, osteoclast activity is not affected in *Fhl2*^{-/-} mice. Next, the bone formation rate was determined *in vivo* by incorporation of calcein into the bone matrix after double injection. The distance between the calcein labels is reflecting osteoblast activity. Importantly, we show that the bone formation rate

is reduced by 24% in *Fhl2*^{-/-} mice (Figure 2C and D). Serum calcium, phosphate, intact PTH, 25-hydroxyvitamin D, estrogen, and testosterone levels as well as alkaline phosphatase activity in *Fhl2*^{-/-} mice are comparable to C57BL/6 wild-type mice (Supplementary Figure 2). Taken together, our data suggest that the osteopenic phenotype of *Fhl2*^{-/-} mice is due to decreased osteoblast function.

Fhl2 expression in osteoblasts regulates bone formation

To further verify that *Fhl2* increases bone formation rate by modulation of osteoblast activity *in vivo*, we generated transgenic FVB mice expressing *Fhl2* specifically in either mature osteoclasts or osteoblasts. Enforced expression of *Fhl2* in osteoblasts results in an increase in bone mass in the transgenic animals by 27% compared to FVB wild-type littermates (Figure 3A and B). The gain in bone mass is caused by an increase in osteoblast activity reflected by an enhanced bone formation rate. Osteoblast and osteoclast numbers remain unchanged (Supplementary Figure 4). In contrast, transgenic mice that express *Fhl2* in osteoclasts neither show a change in bone mass and bone formation rate, nor in osteoclast and osteoblast number (Figure 3A and B, and Supplementary Figure 4). Taken together, these data demonstrate an anabolic function of *Fhl2* in osteoblasts only,

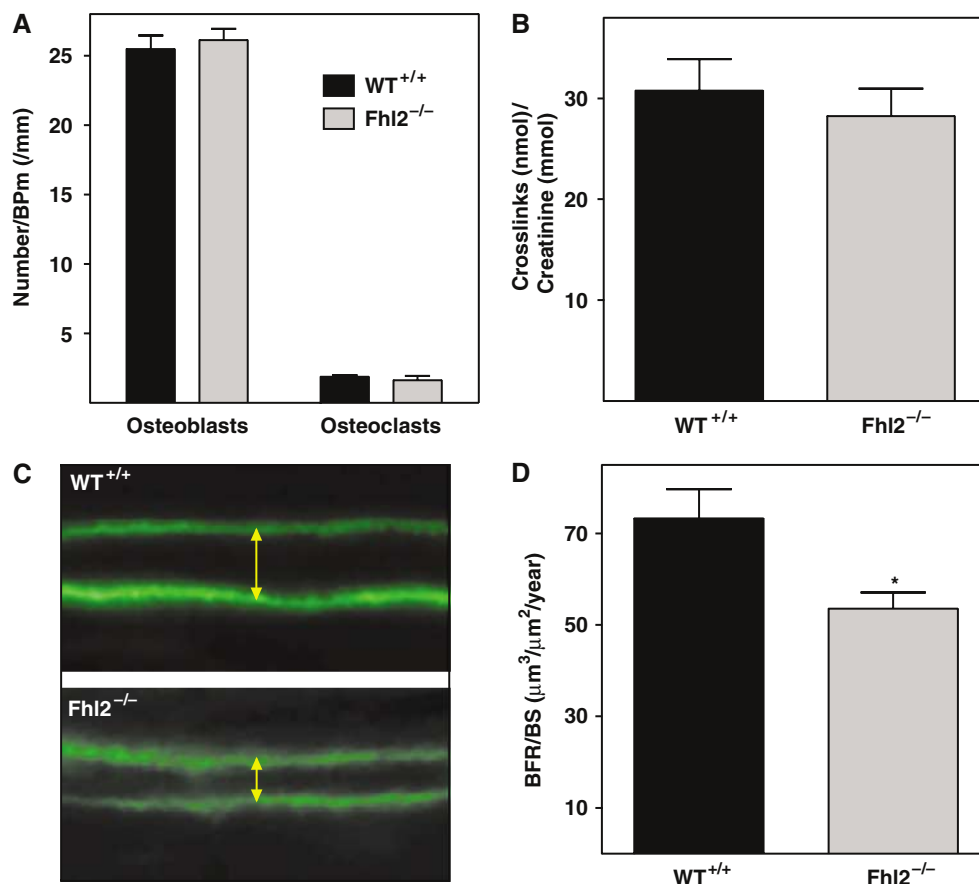


Figure 2 Decreased osteoblast activity in *Fhl2*^{-/-} mice. (A, B) Histomorphometric analysis of osteoblast and osteoclast number per mm bone perimeter (BPm, A) and urinary pyridinium crosslinks as marker of bone resorption (B) display no difference between wild-type and congenic *Fhl2*^{-/-} littermates. (C, D) Bone formation rate was determined *in vivo* by calcein labeling (green). (C) Osteoblast activity is depicted by fluorescent micrographs showing mineralization fronts. Reduced bone formation in *Fhl2*^{-/-} mice is visualized by the decreased distance between both labels (arrows). (D) Quantification of the bone formation rate per bone surface (BFR/BS). Bars represent mean + s.d. ($n \geq 5$). *Statistically significant difference ($P < 0.05$). Analyses were performed in C57BL/6 and *Fhl2*^{-/-} littermates.

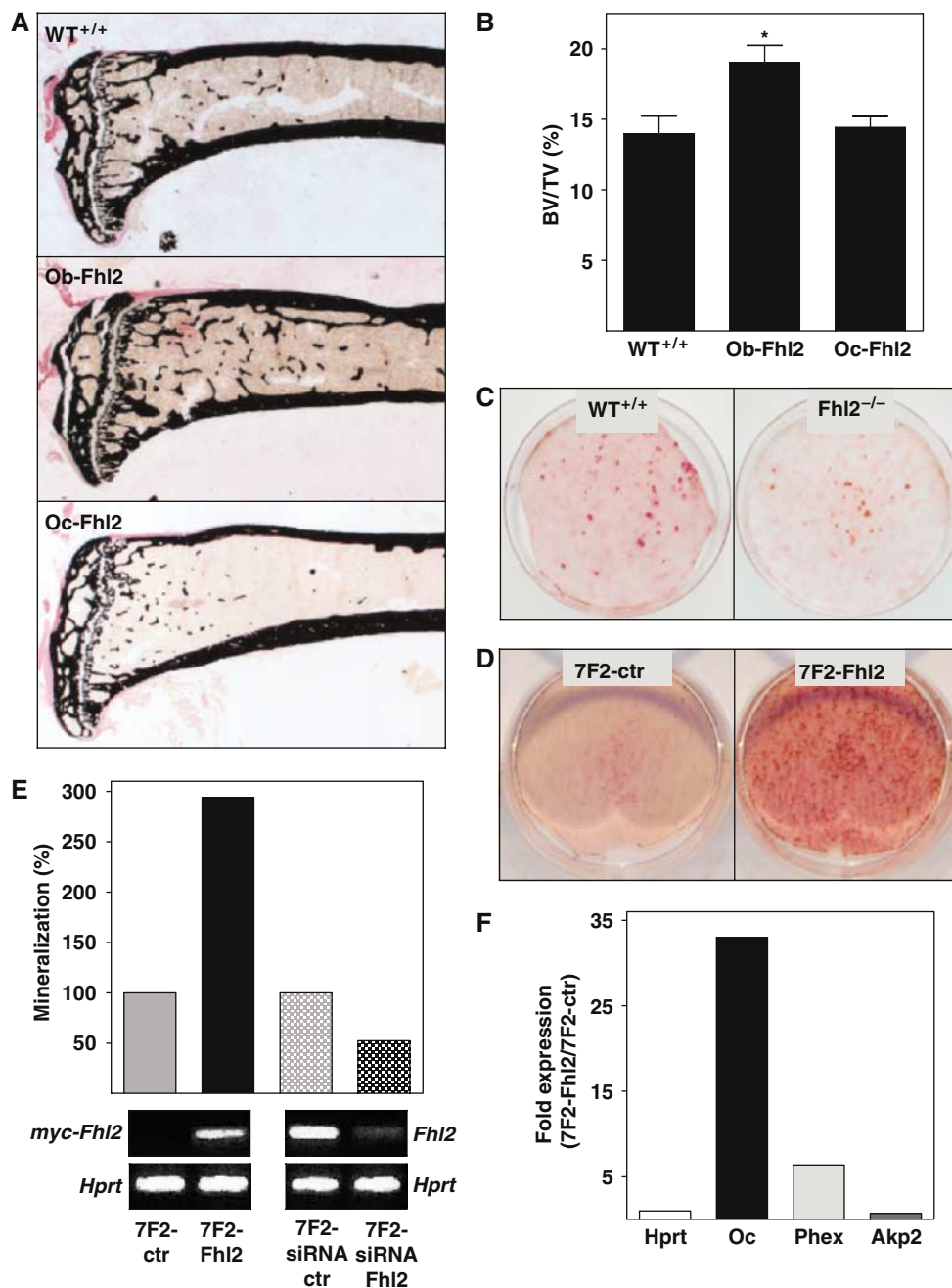


Figure 3 *Fhl2* in osteoblasts controls bone formation. Von Kossa stain (black, **A**) and analysis of bone volume as a ratio of tissue volume (BV/TV) (**B**) of tibiae from wild-type FVB and transgenic FVB littermates expressing *Fhl2* either in osteoblasts (Ob-Fhl2) or osteoclasts (Oc-Fhl2). Bars represent mean + s.d. ($n = 3$). *Statistically significant difference ($P < 0.05$). (**C**) *Ex vivo* primary osteoblast cultures from C57BL/6 wild-type and *Fhl2*^{-/-} mice in mineralization medium. The mineralized matrix, stained with alizarin red S, is decreased in *Fhl2*^{-/-} osteoblasts. (**D**) Stably transfected 7F2-Fhl2 cells and 7F2 control cells (ctr) were stained with alizarin red S for mineralized matrix after 12 days in mineralization medium. (**E**) Mineralization was quantified in genetically modified 7F2 cells and the corresponding controls (ctr). 7F2-Fhl2 cells express myc-tagged *Fhl2* and 7F2-siRNA *Fhl2* cells express siRNA to *Fhl2*. Expression of *myc-Fhl2* and reduction of the endogenous *Fhl2* was verified by RT-PCR. *Hprt* serves as control. (**F**) The ratio of expression of the representative bone markers *Oc*, *Phex*, and *Akp2* was analyzed by qRT-PCR in 7F2-Fhl2 versus 7F2-ctr cells in relation to *Hprt* expression. Experiments were repeated at least three times.

and further support the idea that the osteopenia in *Fhl2*^{-/-} animals is caused by reduced osteoblast activity.

To investigate the consequences of *Fhl2* deficiency on the cellular level, we prepared primary osteoblast cultures derived from calvaria of C57BL/6 wild-type and *Fhl2*^{-/-} mice. Deposition of extracellular matrix was monitored by alizarin red S staining after 17 days in mineralization medium. Importantly, areas of mineralized matrix are reduced in

Fhl2^{-/-} osteoblast cultures (Figure 3C). A time-course reveals that the onset of mineralization and hence differentiation of primary osteoblasts is not delayed in *Fhl2*-deficient cultures (Supplementary Figure 3). The decrease in mineralized area in cultures of primary osteoblasts from *Fhl2*^{-/-} mice demonstrates that the alteration is not caused by endocrine changes, but inherent to the osteoblast lineage and therefore cell autonomous.

If *Fhl2* deficiency is the cause for reduced expression of genes responsible for osteoblast activity and, consequently, for a lower bone formation rate, then augmented *Fhl2* expression should lead to both an increment of marker gene expression and calcified extracellular matrix. To address this issue, we stably transfected the mature osteoblast cell line 7F2 (Thompson *et al*, 1998) with a myc-tagged *Fhl2* expression plasmid (7F2-*Fhl2*). In comparison to control cells, 7F2-*Fhl2* cells exhibit a clear three-fold increase in calcified extracellular matrix already after 12 days in mineralization medium (Figure 3D and E). Moreover, qRT-PCR analyses demonstrate that elevated *Fhl2* expression in 7F2 cells results in increased levels of osteoblast marker genes such as *osteocalcin 2* (*Oc*) and *Phex* (Figure 3F), which are specific for osteoblast activity (Guo and Quarles, 1997; Karsenty and Wagner, 2002). In contrast, expression of *alkaline phosphatase 2* (*Akp2*) reflecting osteoblast differentiation (Aubin *et al*, 1995) is not altered (Figure 3F). Conversely, we reduced endogenous *Fhl2* expression in 7F2 cells by a retroviral-based RNA interference (siRNA). 7F2 cells stably expressing siRNA directed against *Fhl2* (7F2-siRNA *Fhl2*) show reduced calcified extracellular matrix formation by 48% after 12 days in mineralization medium compared to the control cell line expressing an unrelated siRNA (Figure 3E). Marker gene expression is reduced accordingly (data not shown). *Fhl2* expression levels in 7F2-*Fhl2* as well as in the *Fhl2* knockdown cells were verified by RT-PCR (Figure 3E). Taken together, these results demonstrate that the phenotype caused by altered *Fhl2* expression is cell autonomous and that *Fhl2* modulates osteoblast activity.

Fhl2* interacts with *Runx2* and enhances the transcriptional activity of *Runx2

To date, little information is available about the molecular mechanisms regulating the activity of differentiated osteoblasts *in vivo*. It is well known that *Fhl2* can increase the transcriptional activity of the androgen receptor (AR; Müller *et al*, 2002). To evaluate a possible involvement of the AR in the osteopenia caused by *Fhl2* deficiency, mice were continuously treated with 5 α -dihydrotestosterone over a period of 4 weeks. *Fhl2*^{-/-} and C57BL/6 wild-type control animals exhibit an increase in bone mass in an equal ratio (data not shown). These data, together with the observations that both female and male *Fhl2*^{-/-} mice exhibit osteopenia to the same extent (Figure 1), suggest that the interaction of *Fhl2* with AR does not contribute to the observed osteopenia.

Runx2 is known to play a major role in osteoblast function (Ducy, 2000). To demonstrate a possible interaction between *Fhl2* and *Runx2* *in vitro*, we performed pulldown experiments with bacterially expressed GST-*Fhl2*, various mutants thereof, and ³⁵S-methionine-labeled *Runx2* (Figure 4A). *Runx2* interacts with full-length *Fhl2* and the C-terminal LIM domains 3 and 4, but neither with LIM domains 0–2 nor the GST control protein. To determine which region of *Runx2* binds to *Fhl2*, a series of mutant *Runx2* proteins was tested (Figure 4B). Deletion of the *Runx2* N-terminus containing activation domains 1 and 2 does not impair binding to *Fhl2*. Instead, the region containing the RUNT domain as well as the C-terminal activation domain 3 and the repression domain facilitates interaction with *Fhl2* (Figure 4B).

To corroborate the interaction between *Fhl2* and *Runx2* *in vivo*, GST-*Fhl2* and *Runx2* were expressed in 293 cells. The

GST-*Fhl2*/*Runx2* complex was efficiently formed *in vivo* and immobilized on GT-sepharose (Figure 4C). *Runx2* was not found in complexes using GST-transfected control extracts, thus demonstrating specificity (Figure 4C).

To further validate association of *Fhl2* and *Runx2* *in vivo*, 7F2 and primary osteoblast cells were subjected to chromatin immunoprecipitation (ChIP). The *Oc* promoter was chosen because it contains two *Runx2*-binding sites (OSE2; Ducy and Karsenty, 1995). As shown in Figure 4D, genomic DNA corresponding to the proximal *Runx2*-binding site of the osteocalcin promoter was specifically immunoprecipitated with either α -*Runx2* or α -*Fhl2* antibodies. Genomic DNA derived from the *U6* promoter was not enriched, thus demonstrating specificity (Figure 4D). To further demonstrate that *Fhl2* and *Runx2* form a complex on the chromatinized osteocalcin promoter, 7F2 cells and primary osteoblasts were subjected to sequential ChIP (Re-ChIP), first with an α -*Fhl2* antibody and next with either α -*Runx2* or control rabbit IgG. Importantly, the osteocalcin promoter was specifically enriched in an *Fhl2*-dependent manner, demonstrating that *Fhl2* and *Runx2* form a protein complex on the chromatinized osteocalcin promoter *in vivo* (Figure 4D and Supplementary Figure 5). In conclusion, this set of experiments demonstrates association of *Fhl2* and *Runx2* both *in vitro* and *in vivo*.

To examine the potential regulation of *Runx2* by *Fhl2* on a naturally occurring gene, the *Oc* promoter was analyzed because *Runx2* is known to regulate *Oc* expression specifically in mature osteoblasts (Ducy and Karsenty, 1995). As shown in Figure 4E, coexpression of *Fhl2* and *Runx2* significantly enhances reporter gene activity. Mutations in the two OSE2 sites abolishing *Runx2* binding result in a reporter that is neither responsive to *Runx2* (Ducy and Karsenty, 1995) nor *Fhl2* (Figure 4E). Consequently, mutants of *Fhl2*, that do not interact with *Runx2* (Figure 4A), also fail to coactivate reporter gene expression (Figure 4F).

In summary, our data show for the first time the osteopenic phenotype of *Fhl2*^{-/-} mice and unravel the underlying mechanism. We postulate that *Fhl2* is a major regulator of osteoblast function since *Fhl2*^{-/-} mice exhibit decreased osteoblast activity, while transgenic mice with enforced *Fhl2* expression in mature osteoblasts display increased bone mass. Moreover, we show that *Fhl2* functionally interacts with *Runx2*, a regulator of osteoblast activity (Ducy *et al*, 1999). To our knowledge, the *Fhl2*-deficient mouse is the first animal model that exhibits osteopenia caused by a permanently decreased activity of osteoblasts. Thus, modulation of *Fhl2* function by pharmacological intervention offers a novel strategy to prevent bone loss by increasing the anabolic activity of osteoblasts.

Materials and methods

Transgenic mice and histomorphometry

All animals were housed in the pathogen-free barrier facility of the Zentrale Klinische Forschung, Universitätsklinikum Freiburg in accordance with institutional guidelines and approved by the regional board. *Fhl2*^{-/-} mice were bred to a congenic C57BL/6 background (11 or more generations). Transgenic mice were generated by pronuclear injection into the fertilized eggs of FVB mice using standard procedures. Osteoblast- and osteoclast-specific expression of *Fhl2* was driven by a 1.3 kb fragment of the *Oc* promoter (Frendo *et al*, 1998) and a 1.8-kb fragment of tartrate-resistant acid phosphatase promoter (Boyce *et al*, 1995), respectively. Specificity of transgene expression was verified by RT-PCR

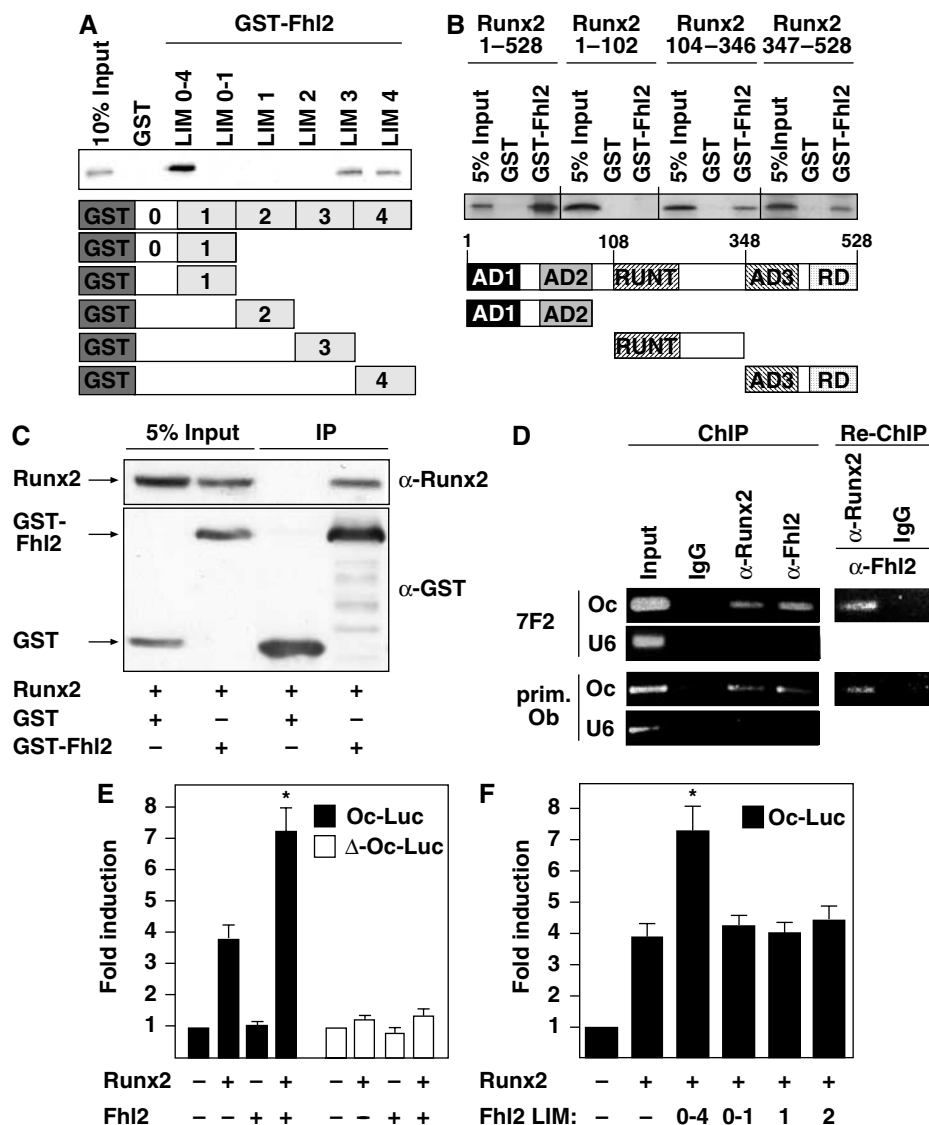


Figure 4 Functional interaction between Fhl2 and Runx2. (A, B) Pull-down assays using GST-Fhl2 or GST-LIM domains, and *in vitro* translated, labeled Runx2 or mutants thereof (AD: activation domain; RD: repression domain; RUNT: DNA-binding domain). (C) *In vivo* GST pull-downs (IP) using lysates from 293 cells transfected with the indicated expression plasmids. Western blots were decorated with either α-Runx2 or α-GST antibodies. Interaction assays were repeated at least three times. (D) Fhl2 and Runx2 form a complex on chromatinized DNA *in vivo*. ChIP or Re-ChIP is performed in 7F2 cells and primary wild-type osteoblasts, with the indicated antibodies or IgG as a control. The precipitated chromatin is amplified by PCR using primers flanking the proximal Runx2-binding site in the osteocalcin promoter. The unrelated U6 promoter serves as a control. (E) As indicated, Runx2 and Fhl2 expression plasmids and the Oc-Luc or ΔOc-Luc (lacking Runx2 binding sites) reporters were cotransfected in MG-63 cells. (F) Transient transfection as in (E) with full-length Fhl2 (LIM 0-4) and indicated mutants thereof. Bars represent mean + s.d. (*n* = 7). *Statistically significant difference (*P* < 0.05).

in three independent lines. Histomorphometry was performed on age- and sex-matched congenic mice (*n* ≥ 3 for each age and gender) as described (Ducy *et al*, 1999). Cryosections of hind legs from 3-day-old mice were incubated for 24 h at 37°C in the dark with buffered X-gal staining solution (Sigma), dehydrated, and mounted. Von Kossa stain was performed as described (Amling *et al*, 1999). Trap stain (Sigma) was performed according to the manufacturer. Mineralization in cell lines was quantified using ImageJ (NIH). All experiments and measurements were repeated at least three times.

Serum markers and proliferation assay

Untreated serum components were analyzed according to the manufacturers: calcium (Sigma) and phosphate (Sigma) related to standards (Randox), intact PTH (ELISA, Immunotopics), 25-hydroxyvitamin D (chemiluminescence assay, Nichols Advantage), alkaline phosphatase activity (Wako), testosterone (RIA, Diagnostic System Laboratories), 17β-estradiol (RIA, Adaltis). Alkaline phos-

phate activity was related to the protein content of serum or cell extracts using Bradford reagent (BioLabs). Measurement of pyridinium crosslinks (EIA, Quidel) was performed according to the manufacturer and related to total urinary creatinine content (Quidel). Proliferation of primary osteoblasts was determined according to the manufacturer (ELISA, Roche). 10⁴ cells/well were seeded in 96-well plates. After 24 h, BrdU was added to the culture medium for 20 h. The analysis was replicated three times with 30 wells for each genotype.

Plasmids

The following plasmids were described: CMX-Fhl2, GST-Fhl2 and mutants thereof (Müller *et al*, 2002), pCMV-Osf2 (Ducy and Karsenty, 1995), Oc-Luc, and ΔOc-Luc (Koeneman *et al*, 1999). To construct the CMX-Runx2 deletion mutants, the corresponding fragments (AD1 + AD2, amino acids 1-102; RUNT, amino acids 104-364; AD3 + RD, amino acids 347-528) were amplified by PCR

and inserted at the *NheI* restriction site of CMX. pIRES-myc-Fhl2-bsd was generated by insertion of myc-Fhl2 cDNA at the *HindIII*/*BamHI* restriction sites of pIRES-bsd. All plasmids were verified by sequencing.

Cell culture and transfections

Primary cells, MG-63, 7F2, and 293 cells were cultured in α -MEM (Cambrex) and DMEM (Cambrex) supplemented with 10% fetal calf serum. Stable 7F2 cell lines, transfected with pIRES-myc-Fhl2-bsd or control plasmid pIRES-bsd, were selected by addition of 10 ng/ μ l blasticidin (Invitrogen). 293 cells were transfected with calcium phosphate, MG-63, and 7F2 cells using Effectene (Qiagen; Müller *et al*, 2000; Metzger *et al*, 2003). Transient transfection assays were carried out in 24-well plates with 5×10^4 cells/well. The total amount of transfected DNA was kept constant (375 ng/well) using 250 ng reporter, 50 ng Runx2, and 15 ng Fhl2 expression plasmids, and the corresponding amounts of empty vectors. Luciferase activity was assayed as described (Müller *et al*, 2000; Metzger *et al*, 2003). All experiments were replicated at least seven times in duplicate. Primary cells were derived from 3- to 5-day-old mice as described (Ducy *et al*, 1999). Starting at confluence, medium was supplemented with 5 mM glycerol 2-phosphate (Sigma) and 100 μ g/ml 2-phospho-L-ascorbic acid (Fluka) every second day for mineralization assays. Primary osteoblasts were infected with a Runx2-expressing retrovirus (pTJ66-Runx2) or the corresponding control virus (Byers *et al*, 2002).

Interactions assays and Western blot analysis

Interaction analyses *in vitro* and *in vivo* were performed as described (Müller *et al*, 2000; Metzger *et al*, 2003). EMSAs were performed as described (Ducy and Karsenty, 1995), with oligonucleotides containing either wild-type (OSE2) or mutant (OSE2mt) Runx2-binding sites. In all, 10 μ g of α -Cbfa1 or M2 (Sigma) was used. Western blots were decorated with α -Fhl2 (1:2000) and α -Runx2 (Santa Cruz, 1:500).

Chromatin immunoprecipitation

ChIP experiments were performed essentially as described using 7F2 cells and primary osteoblasts derived from wild-type mice (Shang *et al*, 2002). Immunoprecipitation was performed with specific antibodies (α -Cbfa1, α -Fhl2) on GammaBindTM-Sepharose 4B (GE-Healthcare). For PCR, 1–5 μ l out of 50 μ l DNA extract was used. For Re-ChIP assays, immunoprecipitations were sequentially washed with TSE I, TSE II, buffer III, and TE (Shang *et al*, 2002). Complexes were eluted by incubation with 10 mM DTT at 37°C for 30 min, diluted 50 times with dilution buffer (Shang *et al*, 2002), followed by a second immunoprecipitation with the indicated antibody. Primer sequences were as follows:

Oc promoter: 5'-AGTCTCCGATGTGGCTCT-3';
5'-CCTCCAGCATCCAGTACAT-3';
U6 promoter: 5'-CACAGACTTGTGGGAGAAGC-3';
5'-GGGTGAGTTTCTTTTGTGC-3'.

Fhl2 knockdown

The siRNA directed against Fhl2 was constructed with the Silencer Express (human H1) siRNA Expression Cassette kit (Ambion) and

subcloned into the lentiviral vector pLV-THM. pLV-THM expressing an unrelated siRNA (#62) served as a control (<http://www.tronolab.unige.ch/>). Sequences for Fhl2 siRNA can be obtained upon personal request.

qRT-PCR and statistical analysis

DNaseI-treated RNA isolated using RNAwiz (Ambion) was used for reverse transcription. Quantitative PCR was performed in an ABI PRISM 7700 sequence detector. Product formation was detected by incorporation of SYBR Green I using ROX as a passive reference (ABgene). The expression ratios of the analyzed cDNAs were related to the normalized C_p of the housekeeping gene *Hprt* in control and sample. Experiments were repeated at least three times. The following primers were used:

Akp2: 5'-AGGGCAATGAGGTCACATCC-3';
5'-GCATCTCGTTATCCGAGTACCAG-3';
Oc: 5'-CTGACCTCACAGATCCCAAGC-3';
5'-TGGTCTGATAGCTCGTCAACAAG-3';
Fhl2: 5'-TTCCCCTCTGCTTTCTTCTACTC-3';
5'-TCCCACTCTCACAGTATTGGC-3';
Hprt: 5'-GTTAAGCAGTACAGCCCCAAA-3';
5'-AGGGCATATCCAACAACAAACTT-3';
myc-Fhl2: 5'-AATTGGAACAAAACACTCTCAGAAGAGGATCTGGA
ATT-3'; 5'-GTAGGCAAAGTCATCGCGA-3';
Phex: 5'-AGCCACTGCTCCACATCTTG-3';
5'-CGGATGAACACAGAATTGCTGTGA-3';
Runx2: 5'-TGTTCTCTGATCGCTCAGTG-3';
5'-GAGGCGTGAATCCATCTTCTG-3'.

Statistical analysis for qPCR was performed by group-wise comparison based on PCR efficiencies and the mean crossing point deviation between the sample and control group using the Relative Expression Software Tool (Pfaffl *et al*, 2002). The *t*-test was used for all other analyses.

Supplementary data

Supplementary data are available at *The EMBO Journal* Online.

Acknowledgements

Fhl2^{-/-} mice were a kind gift from Rhonda Bassel Duby. We thank Thomas Benzinger (pCMV-R8.74, pMD2G-VSVG, pLV-THM), Leland WK Chung (Oc-Luc; Δ -Oc-Luc), Andrés J García (pTJ66; pTJ66-Runx2), Gerard Karsenty (pCMV5-Osf2; pIBS1.3; α -Cbfa1), and G David Roodman (pBSmTRAP) for sharing material, Wolfgang Schäfer, Sibille Ritter, and Michael Hoffmann for the analysis of sex steroids and vitamin D. We appreciate the excellent technical assistance of Lioba Walz and Beate Schmidt and thank the members of the Schüle lab for critical reading of the manuscript. This work was supported by grants from the Deutsche Forschungsgemeinschaft (GU 598/1-1) to TG and (SFB388/C9 and SCHU 688/7-1) to RS.

References

- Amling M, Priemel M, Holzmann T, Chapin K, Rueger JM, Baron R, Demay MB (1999) Rescue of the skeletal phenotype of vitamin D receptor-ablated mice in the setting of normal mineral ion homeostasis: formal histomorphometric and biomechanical analyses. *Endocrinology* **140**: 4982–4987
- Aubin JE, Liu F, Malaval L, Gupta AK (1995) Osteoblast and chondroblast differentiation. *Bone* **17**: 77S–83S
- Boyce BF, Wright K, Reddy SV, Koop BA, Story B, Devlin R, Leach RJ, Roodman GD, Windle JJ (1995) Targeting simian virus 40T antigen to the osteoclast in transgenic mice causes osteoclast tumors and transformation and apoptosis of osteoclasts. *Endocrinology* **136**: 5751–5759
- Byers BA, Pavlath GK, Murphy TJ, Karsenty G, Garcia AJ (2002) Cell-type-dependent up-regulation of *in vitro* mineralization after overexpression of the osteoblast-specific transcription factor Runx2/Cbfa1. *J Bone Miner Res* **17**: 1931–1944
- Chan KK, Tsui SK, Lee SM, Luk SC, Liew CC, Fung KP, Waye MM, Lee CY (1998) Molecular cloning and characterization of FHL2, a novel LIM domain protein preferentially expressed in human heart. *Gene* **210**: 345–350
- Chu PH, Bardwell WM, Gu Y, Ross J, Chen J (2000) FHL2 (SLIM3) is not essential for cardiac development and function. *Mol Cell Biol* **20**: 7460–7462
- Ducy P (2000) Cbfa1: a molecular switch in osteoblast biology. *Dev Dyn* **219**: 461–471
- Ducy P, Karsenty G (1995) Two distinct osteoblast-specific *cis*-acting elements control expression of a mouse osteocalcin gene. *Mol Cell Biol* **15**: 1858–1869
- Ducy P, Starbuck M, Priemel M, Shen J, Pinero G, Geoffroy V, Amling M, Karsenty G (1999) A Cbfa1-dependent genetic pathway controls bone formation beyond embryonic development. *Genes Dev* **13**: 1025–1036

- Ducy P, Zhang R, Geoffroy V, Ridall AL, Karsenty G (1997) *Osf2/Cbfa1*: a transcriptional activator of osteoblast differentiation. *Cell* **89**: 747–754
- Fimia GM, De Cesare D, Sassone-Corsi P (1999) CBP-independent activation of CREM and CREB by the LIM-only protein ACT. *Nature* **398**: 165–169
- Fimia GM, De Cesare D, Sassone-Corsi P (2000) A family of LIM-only transcriptional coactivators: tissue-specific expression and selective activation of CREB and CREM. *Mol Cell Biol* **20**: 8613–8622
- Frendo JL, Xiao G, Fuchs S, Franceschi RT, Karsenty G, Ducy P (1998) Functional hierarchy between two *OSE2* elements in the control of osteocalcin gene expression *in vivo*. *J Biol Chem* **273**: 30509–30516
- Guo R, Quarles LD (1997) Cloning and sequencing of human PHEX from a bone cDNA library: evidence for its developmental stage-specific regulation in osteoblasts. *J Bone Miner Res* **12**: 1009–1017
- Kadmas JL, Beckerle MC (2004) The LIM domain: from the cytoskeleton to the nucleus. *Nat Rev Mol Cell Biol* **5**: 920–931
- Karsenty G, Wagner EF (2002) Reaching a genetic and molecular understanding of skeletal development. *Dev Cell* **2**: 389–406
- Koeneman KS, Yeung F, Chung LW (1999) Osteomimetic properties of prostate cancer cells: a hypothesis supporting the predilection of prostate cancer metastasis and growth in the bone environment. *Prostate* **39**: 246–261
- Komori T, Yagi H, Nomura S, Yamaguchi A, Sasaki K, Deguchi K, Shimizu Y, Bronson RT, Gao YH, Inada M, Sato M, Okamoto R, Kitamura Y, Yoshiki S, Kishimoto T (1997) Targeted disruption of *Cbfa1* results in a complete lack of bone formation owing to maturational arrest of osteoblasts. *Cell* **89**: 755–764
- Kong Y, Shelton JM, Rothermel B, Li X, Richardson JA, Bassel-Duby R, Williams RS (2001) Cardiac-specific LIM protein FHL2 modifies the hypertrophic response to beta-adrenergic stimulation. *Circulation* **103**: 2731–2738
- Labalette L, Renard CA, Neuveut C, Buendia MA, Wei Y (2004) Interaction and functional cooperation between the LIM protein FHL2, CBP/p300, and beta-catenin. *Mol Cell Biol* **24**: 10689–10702
- Lee B, Thirunavukkarasu K, Zhou L, Pastore L, Baldini A, Hecht J, Geoffroy V, Ducy P, Karsenty G (1997) Missense mutations abolishing DNA binding of the osteoblast-specific transcription factor *OSF2/CBFA1* in cleidocranial dysplasia. *Nat Genet* **16**: 307–310
- Metzger E, Müller JM, Ferrari S, Buettner R, Schüle R (2003) A novel inducible transactivation domain in the androgen receptor: implications for PRK in prostate cancer. *EMBO J* **22**: 270–280
- Morlon A, Sassone-Corsi P (2003) The LIM-only protein FHL2 is a serum-inducible transcriptional coactivator of AP-1. *Proc Natl Acad Sci USA* **100**: 3977–3982
- Müller JM, Isele U, Metzger E, Rempel A, Moser M, Pscherer A, Breyer T, Holubarsch C, Buettner R, Schüle R (2000) FHL2, a novel tissue-specific coactivator of the androgen receptor. *EMBO J* **19**: 359–369
- Müller JM, Metzger E, Greschik H, Bosserhoff AK, Mercep L, Buettner R, Schüle R (2002) The transcriptional coactivator FHL2 transmits Rho signals from the cell membrane into the nucleus. *EMBO J* **21**: 736–748
- Mundlos S, Otto F, Mundlos C, Mulliken JB, Aylsworth AS, Albright S, Lindhout D, Cole WG, Henn W, Knoll JH, Owen MJ, Mertelsmann R, Zabel BU, Olsen BR (1997) Mutations involving the transcription factor CBFA1 cause cleidocranial dysplasia. *Cell* **89**: 773–779
- Otto F, Thornell AP, Crompton T, Denzel A, Gilmour KC, Rosewell IR, Stamp GW, Beddington RS, Mundlos S, Olsen BR, Selby PB, Owen MJ (1997) *Cbfa1*, a candidate gene for cleidocranial dysplasia syndrome, is essential for osteoblast differentiation and bone development. *Cell* **89**: 765–771
- Pfaffl MW, Horgan GW, Dempfle L (2002) Relative expression software tool (REST) for group-wise comparison and statistical analysis of relative expression results in real-time PCR. *Nucleic Acids Res* **30**: e36
- Philippart U, Schratz G, Dieterich C, Müller JM, Galgoczy P, Engel FB, Keating MT, Gertler F, Schüle R, Vingron M, Nordheim A (2004) The SRF target gene *Fhl2* antagonizes RhoA/MAL-dependent activation of SRF. *Mol Cell* **16**: 867–880
- Purcell NH, Darwis D, Bueno OF, Müller JM, Schüle R, Molkentin JD (2004) Extracellular signal-regulated kinase 2 interacts with and is negatively regulated by the LIM-only protein FHL2 in cardiomyocytes. *Mol Cell Biol* **24**: 1081–1095
- Robins SP, Black D, Paterson CR, Reid DM, Duncan A, Seibel MJ (1991) Evaluation of urinary hydroxypyridinium crosslink measurements as resorption markers in metabolic bone diseases. *Eur J Clin Invest* **21**: 310–315
- Shang Y, Myers M, Brown M (2002) Formation of the androgen receptor transcription complex. *Mol Cell* **9**: 601–610
- Teitelbaum SL (2000) Bone resorption by osteoclasts. *Science* **289**: 1504–1508
- Thompson DL, Lum KD, Nygaard SC, Kuestner RE, Kelly KA, Gimble JM, Moore EE (1998) The derivation and characterization of stromal cell lines from the bone marrow of *p53*^{-/-} mice: new insights into osteoblast and adipocyte differentiation. *J Bone Miner Res* **13**: 195–204
- Yang Y, Hou H, Haller EM, Nicosia SV, Bai W, Labalette C, Renard CA, Neuveut C, Buendia MA, Wei Y (2005) Suppression of FOXO1 activity by FHL2 through SIRT1-mediated deacetylation. *EMBO J* **24**: 1021–1032